

A Random PWM with Constant Common-Mode Voltage for PV Inverter

R. Ganesh Kishore

PG Scholar

*Department of Electronics & Communication Engineering
Christian College Of Engineering & Technology,
Dindigul Tamilnadu-624619 India*

D. Thalpathi Udhayakumar

Research scholar

*Department of Electronics & Communication Engineering
Christian College Of Engineering & Technology,
Dindigul Tamilnadu-624619 India*

Abstract

This paper presents a Random Pulse Width Modulation (RPWM) full bridge transformer-less photovoltaic inverter technique brings low Total Harmonics Distortion (THD). In better elimination of THD induced by the common-mode voltage, a clamping technology has the ability to hold the common-mode voltage on a constant value in the freewheeling period. The passive clamping technology consists of two diodes and a capacitor divider at the dc side of full bridge inverter topology of constant common-mode voltage (FB-CCV). RPWM technique is fed into FB-CCV. MOSFET switches are been employed in ac side because of its low switching losses. RPWM is a new and effective technique which possesses low acoustic noise and mechanical vibrations and it is suitable for many applications such as industrial motor drives and electric vehicles in which interference with neighboring equipment and environment is minimized. The performance of this modulation is simulated in Plexim/Simulink environment, to measure the THD and the results are obtained.

Keywords: Random Pulse Width Modulation (RPWM), constant common-mode voltage, Total Harmonics Distortion (THD)

I. INTRODUCTION

Renewable energy sources are getting more and more widespread mainly due to the fact that they are environmentally friendly. The reduced prices of Photovoltaic (PV) system components and technological developments of power electronics have also motivated the harnessing of renewable energy. Furthermore, renewable energy is independent of limited fossil and nuclear fuels and thus it has the potential to be a sustainable energy source for the future. There is a strong trend in PV inverter technology to use transformer-less grid-connected topologies. Transformer-less topologies eliminate the Line Frequency Transformer from grid-connected PV systems. This results in reduced cost, physical size and weight of the inverter. The other advantage is an increase in the overall power efficiency and improved power factor at light loads. The elimination of the transformer, however, creates challenges which the PV system has to mitigate. Among these challenges is the need to provide galvanic isolation between the PV generator and the connected grid. For other inverters, the galvanic isolation is provided by the transformer. In these conditions, common-mode currents can appear through the stray capacitance between the PV array and the ground. The other challenge introduced by transformer-less topologies, is the danger of dc injection in to the grid. Dc in an ac system causes saturation of distribution transformers in the network and also affects the accuracy of Instrument transformers and energy meters. The choice of a transformer-less topology is thus critical in ensuring that the undesirable operational effects are minimized to acceptable levels while achieving the benefits of using the topology as outlined earlier. Information was researched on the various components of the PV inverter systems starting from the principle of operation of a solar cell, PV module characteristics, components of PV modules and their manufacture, the optimization of PV input-source through the use of Maximum Power Point Trackers (MPPT) as well as associated components such as storage devices like batteries. Grid-connected PV systems produce large quantities of photovoltaic electricity in a single point. The size of PV systems ranges from several hundred kilowatts to several megawatts. These applications are located on large industrial buildings such as airport terminals or railway stations.

There are two main topology groups used in case of grid connected PV systems and they are

- 1) With galvanic isolation – Galvanic isolation can be done on the DC side, in the form of a high frequency DC-DC transformer or on the grid side in the form of a big-bulky AC transformer.
- 2) Without galvanic isolation- Here, the transformer is omitted and is called as transformer-less topology.

The absence of transformer leads to the reduction of transformer losses and thus improved efficiency of the system by 1-2%. As no inductive reactance contribution from the transformer, thus improved power factor for low loading.

PV requires minimal maintenance. Solar modules are almost maintenance free and offer easy installation. PV systems are extremely safe and highly reliable. The estimated lifetime of a PV module is 30 years. PV system operates in two different modes: grid-connected mode and island mode. In the grid-connected mode, maximum power is extracted from the PV system to supply maximum available power into the grid. Single- and two-stage grid-connected systems are commonly used topologies in

single- and three-phase PV applications. In a single-stage grid-connected system, the PV system utilizes a single conversion unit (dc/ac power inverter) to track the maximum power point (MPP) and interface the PV system to the grid.

This paper is organized as follows. Section II presents the circuit configuration and operation principle of the FB-CCV. The Random Pulse Width Modulation technique presented in Section III. The simulation models and experimental results are shown in Section IV to explore the performance of the FBCCV. Section V summarizes the conclusions drawn from the investigation.

II. STRUCTURE AND OPERATION PRINCIPLE

A. Circuit Configuration

FB-CCV is an advanced model of Highly Efficient and Reliable Inverter Concept (HERIC) topology. The components used in the FB-CCV are PV panel which is used to extract the solar radiations from the environment. The passive clamping branches consist of a capacitor divider and two diodes. They are added into the dc side and two unidirectional freewheeling branches which consist of a set of MOSFET switches are added into the ac side of the FB-CCV. Two sets of IGBT switches are employed as main and two MOSFET switches are employed as freewheeling switches. Both main and freewheeling switches are ideal switches with anti-parallel diodes and the power diodes are also ideal diodes. Moreover the capacitance C_{dc1} and C_{dc2} of the dc filter are to be treated as constant voltage sources.

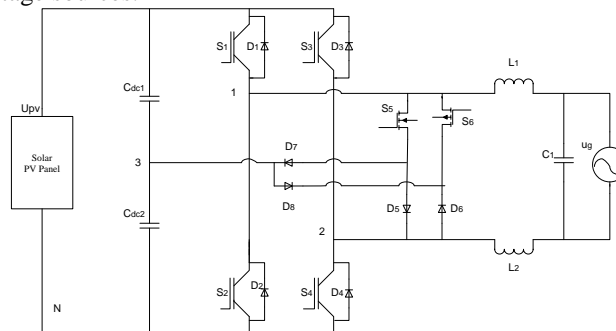


Fig. 1: FB-CCV topology

Fig 1 shows the structure of FB-CCV topology. In the positive half period of the grid-in current, the operation style of $S1$ and $S4$ is in RPWM modulation, $S2$ and $S3$ are always OFF. The switches $S5$ and $S6$ are complementary with the switches $S1$ and $S4$ with a dead time to avoid the short-circuit paths from $S1, S5, D5, S4$ and $S1, S5, D7$ respectively. In the negative half period of the grid-in current, the operation style of $S2$ and $S3$ is in RPWM modulation, $S1$ and $S4$ are always OFF. The switches $S5$ and $S6$ are complementary with the switches $S2$ and $S3$ with a dead time to avoid the short-circuit paths from $S3, D6, S6, S2$ and $D8, S6, S2$ respectively.

B. Operation Principle

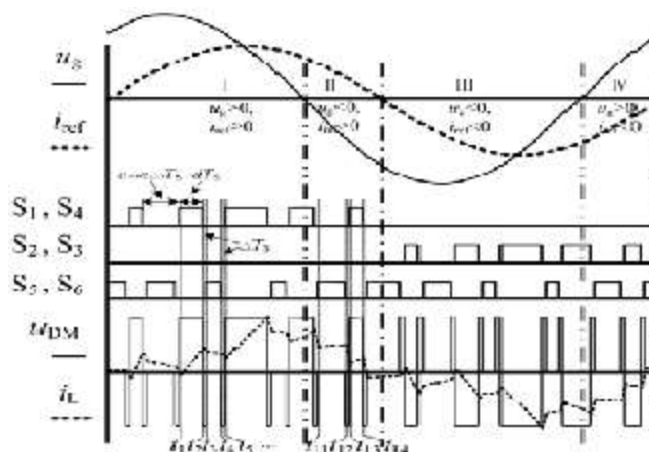


Fig. 2: Operation waveforms of the FB-CCV with RPWM.

The above waveform shows the operation of FB-CCV with RPWM. Generally in RPWM style two freewheeling modes exists in the freewheeling period. One is dead-time mode and another is zero-vector mode. For dead-time mode the time intervals are $[t_2, t_3]$ and $[t_4, t_5]$ and for zero-vector mode the time interval is $[t_3, t_4]$.

Fig.2 has RPWM has four states of operation modes. They are

- 1) State I ($u_g > 0$ and $i_{ref} > 0$),

- 2) State II ($u_g < 0$ and $i_{ref} > 0$),
- 3) State III ($u_g < 0$ and $i_{ref} < 0$) and
- 4) State IV ($u_g > 0$ and $i_{ref} < 0$).

Each state has three kinds of stages. The switching modes in the positive half period of the grid-in current are equal to the negative half period. In state I, both the grid voltage and the grid current stays in positive cycle.

The first stage of state I is $[t_1, t_2]$ at t_1 , the main switches S_1 and S_4 are turned ON and other switches are turned OFF, and the inductor current i_L is equal to $I_L(t_1)$. In this stage, the power flow occurs from the PV side to the grid through main switches S_1 , S_4 and the filter. The inductor current i_L increases linearly from t_1 to t_2 . Hence this stage is named as power mode.

$$i_L(t) - I_L(t_1) = \frac{U_{pv} - u_g}{L}(t - t_1) \quad \text{---- (1)}$$

$$u_{12} = U_{pv} \quad \text{---- (2)}$$

In Stage I-2 $[t_2, t_3]$ at t_2 the main switches S_1 and S_4 are turned OFF while all switches are turned off. Hence this stage is known as dead-time freewheeling mode. The inductor current i_L flows to the anti-parallel diodes D_2 and D_3 and to a dc bus capacitor. The inductor current i_L reduces linearly due to the effects of the PV voltage and the grid voltage.

$$i_L(t) - I_L(t_2) = \frac{-U_{pv} - u_g}{L}(t - t_2) \quad \text{---- (3)}$$

$$u_{12} = -U_{pv} \quad \text{---- (4)}$$

The third stage of state I is $[t_3, t_4]$ at t_3 , the freewheeling switches S_5 and S_6 are turned ON and the other main switches are turned OFF. As the freewheeling switches alone are turned ON, this stage is called as zero-vector freewheeling mode. The inductor current i_L flows through the diode D_6 and to the switch S_6 . The inductor current i_L reduces linearly due to the effect of the grid voltage.

$$i_L(t) - I_L(t_3) = \frac{-u_g}{L}(t - t_3) \quad \text{---- (5)}$$

$$u_{12} = 0 \quad \text{---- (6)}$$

At t_4 , the freewheeling switches S_5 and S_6 are turned OFF and then all the main switches are turned OFF. The inverter works at the dead-time freewheeling mode again which is similar to the second stage of state I.

In state II, the grid voltage goes to negative half period and the grid current still stays at positive cycle. State II has 3 different kinds of stages.

The first stage of state II is $[t_{11}, t_{12}]$ at t_{11} , the freewheeling switches S_5 and S_6 are turned ON and other main switches are turned OFF. The direction of the grid voltage is reversed from positive to negative half period. The inductor current i_L flows through the diode D_6 and the switch S_6 . The inductor current i_L is linearly increased due to the effect of the grid voltage. This stage is known as the energy storage mode.

$$i_L(t) - I_L(t_{11}) = \frac{|u_g|}{L}(t - t_{11}) \quad \text{---- (7)}$$

$$u_{12} = 0 \quad \text{---- (8)}$$

In stage II-2 $[t_{12}, t_{13}]$ at t_{12} , the freewheeling switches S_5 and S_6 are turned OFF and other main switches are turned OFF. The inductor current i_L flows from the grid to the dc bus capacitor through the anti-parallel diodes D_2 and D_3 . The inductor current i_L reduces linearly due to the effects of the difference of the PV voltage and grid voltage.

$$i_L(t) - I_L(t_{12}) = \frac{-U_{pv} + |u_g|}{L}(t - t_{12}) \quad \text{---- (9)}$$

$$u_{12} = -U_{pv} \quad \text{---- (10)}$$

The third stage of state II is $[t_{13}, t_{14}]$ at t_{13} , the main switches S_1 and S_4 are turned ON and other switches are turned OFF. The energy is stored in filter inductors through S_1 and S_4 in this stage. The inductor current i_L is increased linearly till t_{14} .

$$i_L(t) - I_L(t_{13}) = \frac{U_{pv} + |u_g|}{L}(t - t_{13}) \quad \text{---- (11)}$$

$$u_{12} = U_{pv} \quad \text{---- (12)}$$

Table - 1

Analysis of Device Operation in FB-CCV Topology

	Device type	FB-CCV
Number	MOSFET	2
	IGBT	4
	Diode	4
Turn on/off loss	MOSFET	1
	IGBT	2
Conduction loss	MOSFET	0
	IGBT	2
Freewheeling loss	MOSFET	1
	IGBT	0
	Diode	1
Reverse recovery loss	Diode	2
Gate loss	MOSFET	2
	IGBT	2

Table 1 shows the operation of device in FB-CCV topology. In both the differential-mode current, i_{DM} and common-mode current, i_{CM} cases, the potential of the freewheeling path can be freely clamped to $0.5 \cdot U_{PV}$. The clamping process in the negative half period of the grid current is similar with the positive half period of the grid current.

Keep the negative terminal N of PV solar panels as the reference, the midpoints 1 and 2 of the bridge legs are output terminals. According to the definition of differential mode voltage, the differential mode voltage v_{DM} is related to v_{1N} and v_{2N} . The differential mode voltage of the FB-CCV has three kinds of levels. They are U_{pv} , $-U_{pv}$ and 0 in each switching period. The grid current of the FB-CCV flows through only two power devices in all the 3 Stages. The zero-vector conduction loss of the MOSFET +diode freewheeling paths of the FB-CCV is less than of the IGBT + diode. In order to reduce the total power loss, a full MOSFET is paralleled to form the zero-vector freewheeling path. Here full MOSFET is referred the diodes are replaced by MOSFET.

$$u_{DM} = u_{1N} - u_{2N} = u_{12} \text{ ---- (13)}$$

The voltage common to both the input terminal of a device with respect to output reference is known as common mode voltage and this states the common mode Characteristics. According to the definition of the common mode voltage, u_{CM} is related to u_{1N} and u_{2N} and termed in the following,

$$u_{CM} = \frac{u_{1N} + u_{2N}}{2} \text{ ---- (14)}$$

III. RANDOM PULSE WIDTH MODULATION

RPWM is the most effective method to Randomizing the switching frequency. The PWM scheme based on the use of “nondeterministic” random number generation has been developed to generate Random PWM waveforms for dc-ac power conversion applications. Random PWM technique has been introduced by A.M Trzynadlowski, R.L kirlin and S.Legoski in the year 1987. Randomized Switching Frequency, Randomized Pulse Position and Random Switching are the basic RPWM strategies.

This RPWM approach is suitable for many applications such as industrial motor drives and electric vehicles in which interference with neighboring equipment and environment should be minimized. The unique effects of RPWM are, it automatically drops small pulses which lead to improve efficiency and neglect lower order harmonics. RPWM techniques for voltage-controlled power electronic inverters that have been attracting an increasing interest due to the unique effects of these techniques on the inverter supplied drive systems.

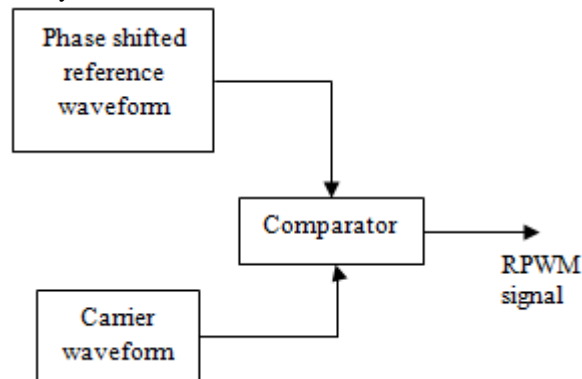


Fig. 3: Generation of the Random PWM.

The reference signal is phase shifted to 120° and 240° . Then it is compared with a carrier signal. These two signals are compared in a comparator and random pulse width modulation signal is generated. This is shown in the fig 3. This phase shift is done by the transport delay of the sinusoidal reference signal. In random switching technique, the randomly generated fractional numbers having uniform probability distribution are compared with the desired duty ratios. Random switching frequency has been found to be the most effective method of RPWM. The random PWM strategy is divided into two separate sequences that divide the switching cycles respect to positive and negative cycles which control the current flow of the inverter. Most of the RPWM schemes for DC-AC power converters usually work well with high-sampling frequency. RPWM is a technique that cannot be controlled by any control schemes. The digital implementation of this scheme has a significant effect on sampling frequencies and it is limited by the speed of processors used. Various RPWM schemes have been implemented digitally using microcontrollers, DSPs and FPGAs. The power carried by the RPWM signal is no longer limited to a few leading frequency that are normally controlled by the switching frequency.

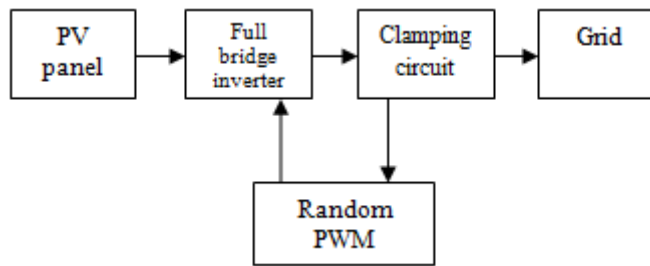


Fig. 4: Block diagram representation of RPWM methodology.

The Block diagram representation of RPWM methodology is shown in the fig 4. PV panel extracts the solar radiations of sun from the environment. The output of the PV panel is dc and it is converted into ac by the full bridge inverter. A clamping technology has the ability to hold the common mode voltage on a constant value with the help of Random PWM and the filtered ac power is given to the grid.

IV. SIMULATION AND EXPERIMENTAL RESULTS

Installing the PLECS Blockset on the system is easy and no need to have system administrator permissions to install. PLECS is the product of PLEXIM. Moreover PLECS is the tool for high-speed simulations of power electronic systems. The version plects 3.6 is used in this experiment. In order to validate the performance of the inverter a model is been built using the Plexim software tool. The elements of plexim are mainly used in Electrical and Electronics circuits. This is the main advantage of Plexim software tool. This software has many basic elements such as scope, display, probe, transformers, switches, power semiconductors, passive elements, ac and dc machines and power modules. Plexim GmbH or Plexim, is providing simulation software for power electronic systems.

The product PLECS is used for product development in power electronics. PLECS enhances Simulink with the capability to simulate electrical circuits directly. At Simulink block level the circuit is represented as a subsystem, so the user can build controls and take full advantage of the Simulink environment and its toolboxes. PLECS Blockset users can take advantage of the entire Simulink library and the various extensions to model special controls or other physical domains. The concept of integration into Simulink has the advantage that only the part of the system in which electrical units are of interest needs to be modeled as an electrical circuit. The area of application includes renewable energy, automotive, aerospace, industrial, traction drives, and power supplies. Their official Website is www.plexim.com. The results and experimental values are concluded below. The harmonic reduction ability of the RPWM is validated by the simulation study.

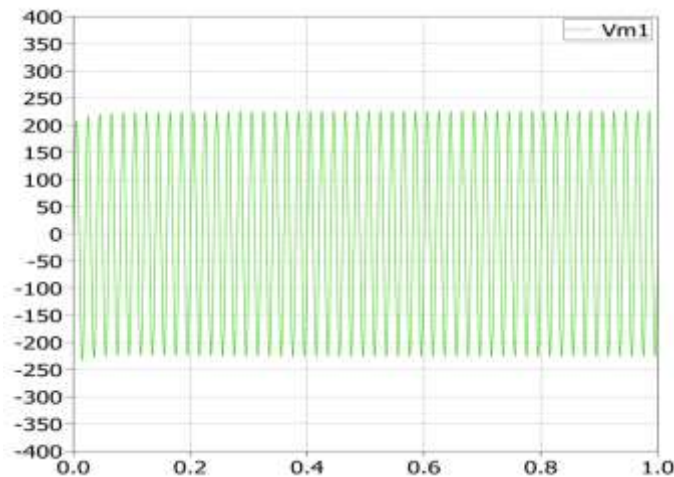


Fig. 5: Grid in voltage

The above figure shows the waveform of grid in voltage in of random PWM technique in PLEXIM tool which is implemented in FB-CCV topology. Sinusoidal and triangular waves are taken as reference and carrier signals respectively. By using transport delay tool phase shifting of reference signal is done.

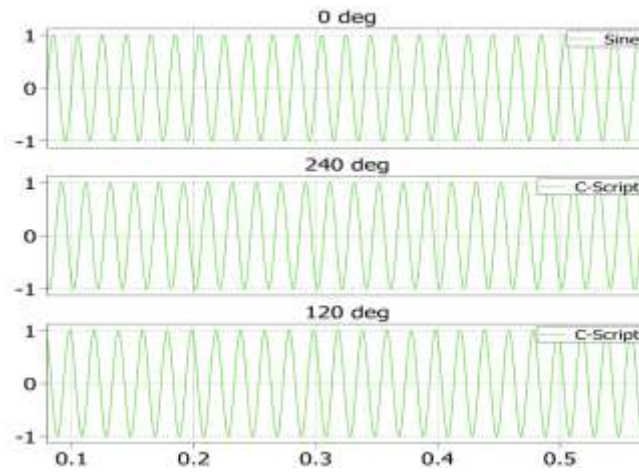


Fig. 6: Phase shifting of reference sine wave

From fig. 6, 0° , 120° and 240° represents the phase shift of sinusoidal reference signal. These three waveforms combined together and random PWM technology is formed.

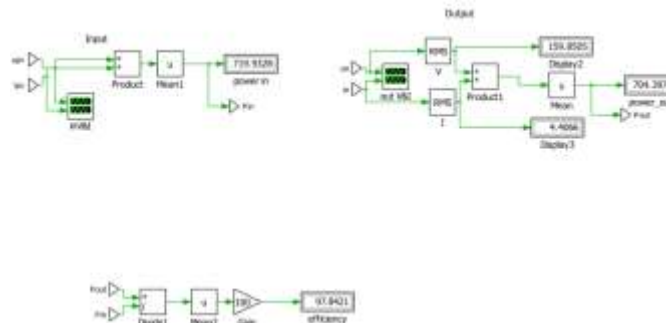


Fig. 7: Efficiency and Output power of RPWM

The above figure shows the representation of Efficiency and Output power of RPWM technique of FB-CCV topology. Efficiency is 97.8% and output power in the grid is 704.3 watts.

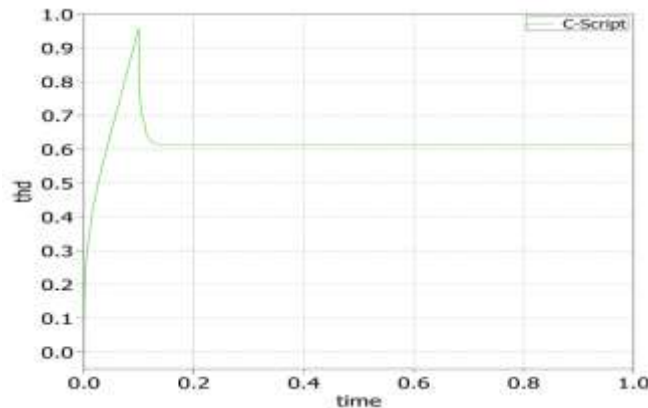


Fig. 8: THD of Random PWM

Table - 2
Parameters and Its Data of R PWM.

S.No	PARAMETERS	RPWM
1	Output Power	704.3 W
2	THD	61.2%
3	Efficiency	97.8 %

V. CONCLUSION

Experimental results show that the level of Total Harmonic Distortion in the system is reduced to 61.2%. This shows the high conversion efficiency and low THD. A RPWM full-bridge inverter topology with two unidirectional freewheeling branches and a passive clamping branch has been discussed in this paper. The inverter has the two operation modes in the freewheeling period.

They are dead-time freewheeling mode and zero-vector freewheeling mode. It guarantees that the high frequency common mode voltage is on a constant value in whole switching period. The experiments have conformed the effectiveness of random PWM technique

REFERENCES

- [1] Hua F. Xiao, Member, IEEE, Ke Lan, and Li Zhang (Jun. 2015), "A Quasi-Unipolar SPWM Full-Bridge Transformerless PV Grid Connected Inverter With Constant Common-Mode Voltage," *IEEE TRANSACTIONS ON POWER ELECTRONICS*, VOL. 30, NO. 6, pp. 3122-3132
- [2] L. Zhang, K. Sun, Y. Xing, and M. Xing (Mar 2014), "H6 transformerless full-bridge PV grid-tied inverters," *IEEE Trans. Power Electron.*, vol. 29, no. 3, pp. 1229–1238.
- [3] B. N. Alajmi, K. H. Ahmed, G. P. Adam, and B. W. Williams (Jun. 2013), "Single phase single-stage transformerless grid-connected PV system," *IEEE Trans. Power Electron.*, vol. 28, no. 6, pp. 2664–2676.
- [4] Z. Zhao, Y. Zhong, H. Gao, L. Yuan, and T. Lu (Mar. 2012) , "Hybrid selective harmonic elimination PWM for common-mode voltage reduction in three level neutral-point-clamped inverters for variable speed induction drives," *IEEE Trans. Power Electron.*, vol. 27, no. 3, pp. 1152–1158.
- [5] C.-C. Hou, C.-C. Shih, P.-T. Cheng, and A. M. Hava (Apr. 2013), "Common-mode voltage reduction pulsewidth modulation techniques for three-phase gridconnected converters," *IEEE Trans. Power Electron.* vol. 28, no. 4, pp. 1971–1979.
- [6] Duran M. J., J. Prieto, and F. Barrero (Aug. 2013), "Space Vector PWM with reduced common-mode voltage for five-phase induction motor drives operating in over modulation zone," *IEEE Trans. Power Electron.*, vol. 28, no. 8, pp. 4030–4040
- [7] Koutroulis E. and F. Blaabjerg (Jan. 2013), "Design optimization of transformerless grid-connected PV inverters including reliability," *IEEE Trans. Power Electron.*, vol. 28, no. 1, pp. 325–335.
- [8] Shin J. -W., H. Shin, G. -S. Seo, J. -I. Ha, and B. -H. Cho (Apr. 2013), "Lowcommon mode voltage h-bridge converter with additional switch Legs," *IEEE Trans. Power Electron.*, vol. 28, no. 4, pp. 1773–1782.
- [9] Xiao H. F and S. J. Xie (Apr. 2012), "Transformerless split-inductor neutral point clamped three-level PVgrid-connected inverter," *IEEE Trans. Power Electron.*, vol. 27, no. 4, pp. 1799–808.
- [10] Zhu N, D. Xu, B.Wu, N. R. Zargari, M. Kazerani, and F. Liu (Feb. 2013), "Commonmode voltage reduction methods for current-source converters in medium voltage drives," *IEEE Trans. Power Electron.*, vol. 28, no. 2, pp. 995–1006.